On-Chip Optical Sampling using an Integrated SOA-based Nonlinear Optical Loop Mirror

Leimeng Zhuang[1], Chen Zhu[1], Bill Corcoran[1,2], Zihan Geng[1], Binhuang Song[1], and Arthur Lowery[1,2]

[1] Electro-Photonics Laboratory, Department of Electrical and Computer Systems Engineering, Monash University, Clayton, VIC 3800, Australia (leimeng.zhuang@monash.edu)
[2] Centre of Ultrahigh bandwidth Devices for optical systems (CUDOS), Monash University, Australia

Abstract we report the first demonstration of on-chip optical sampling using an integrated SOA-based nonlinear optical loop mirror. The device implements a compact design featuring a size of 2 x 1.2 mm^2 and a sampling window of ≈ 30 ps.

Introduction

Optical sampling is an important function for high-capacity transmission techniques, such as all-optical orthogonal frequency division multiplexing (OFDM)[1] and optical time division multiplexing (OTDM)[2]. It allows a data tributary to be reproduced without interference from other data tributaries (i.e. inter-carrier-interference in OFDM signals or inter-symbol-interference in OTDM signals). In effect, performing optical sampling lowers the required receiver electrical bandwidth: without it, this bandwidth has to exceed the combined baud rate of many data tributaries.

To date, several approaches to perform optical sampling have been investigated. For example, (a) using electro-optical modulators as sampling gates[3]; (b) using nonlinear photonic devices to mix the signal with a sampling pulse train[4]. Owing to the fast-responses of optical nonlinear phenomena, the latter category has demonstrated picosecond-level sampling. For the implementation of such an optical sampler, utilizing the cross-phase modulation (XPM) effect in semiconductor optical amplifiers (SOAs) is a widely-investigated practice due to its advantages of easy operation, high power-efficiency, and simultaneous signal amplification[5]. To perform sampling operation, the SOAs are commonly incorporated in interferometer structures to convert the SOA-based signal phase modulation to the signal intensity switching effect. A typical example is the SOA-based Mach-Zehnder interferometer (SOA-MZI), a previous work of which has demonstrated a sampling window of 1 ps[4]. However, the construction of such devices requires two SOAs and two couplers for the input and output of the signal. A simpler device configuration is the SOA-based Sagnac-loop interferometer, which requires only one SOA and one coupler to form a nonlinear optical loop mirror (SOA-NOLM). One example, known as the terahertz optical asymmetric demultiplexer (TOAD)[6], is a promising candidate for implementing ultrafast optical sampling, where the SOA is placed asymmetrically in the loop and is able to provide a sampling window in the order of the time delay determined by the position offset of the SOA from the loop midpoint.

Conventional implementations of SOA-NOLMs/TOADs are bulky, having their optical paths implemented using optical fibres. In addition, SOAs that are short relative to their position offset are used, so that the delay of the SOA has an insignificant effect on the sampling window. Implementing such devices in photonic integrated circuits miniaturizes their sizes and provides robust operation with low-cost potential. These features are highly desired for realizing compact OFDM and OTDM receivers.

In this paper, we report an on-chip optical sampler using an integrated SOA-NOLM. Unlike the conventional designs, we use a relatively long SOA for the benefit of signal gain, and manipulate the sampling window width with the loop roundtrip delay. In a proof-of-concept experiment, we show that such a device using a 1-mm SOA is able to be fabricated with a chip size of 2 x 1.2 mm^2 and provide a sampling window of ≈ 30 ps.

Device description

Figure 1 shows the SOA-NOLM chip. The chip is fabricated in an Indium Phosphide (InP) waveguide platform[7], by JePPIX's SMART Photonics foundry service. The circuit is based on shallow-etched InP waveguide with a propagation loss of 3.5 dB/cm, coupler insertion loss of 1 dB, and fibre-coupling loss of about 4 dB/facet using tapered fibres. The SOA uses a

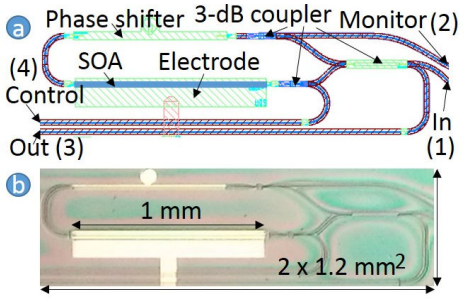

Fig. 1: The SOA-NOLM chip: (a) mask layout, (b) photomicrograph.

ISBN 978-3-8007-4274-5

polarization-insensitive InGaAsP/InP quantum well with an active area of 1000 × 2 μm², giving a time delay ≈ 10 ps and a small-signal gain of 8 dB for a forward bias current of 7 kA/cm² at a wavelength around 1550 nm. The loop has a round trip delay ≈ 23 ps. Two 3-dB tap-out ports for control signal insertion and power monitoring, and a phase shifter for test purposes. The device size is 2 × 1.2 mm².

Figure 2 illustrates the general working principle of the device as an optical sampler. As indicated in a schematic in Fig. 2a, the input signals to be sampled can be applied to either of the two coupler ports, and a control pulse is inserted into the SOA via an additional port within the loop. Owing to the XGM effect in the SOA and its asymmetric position in the loop, the control pulse varies the phases of the counter-propagating signals at different times. This time difference is illustrated in Fig. 2b, where an equivalent schematic using a SOA-MZI architecture is shown, having the signal co-propagating with the control pulse in the upper arm and counter-propagating in the lower arm. In a simplified model, we can assume that the SOA behaves like a travelling-wave phase modulator; however, at any position along the SOA, when a control pulse passes (Fig. 2c), the XGM-induced time-domain phase response at that position would feature a fast rising edge due to the short SOA saturation time, but a slow falling edge due to the SOA carrier recovery time (Fig. 2d). The eventual phase changes of the counter-

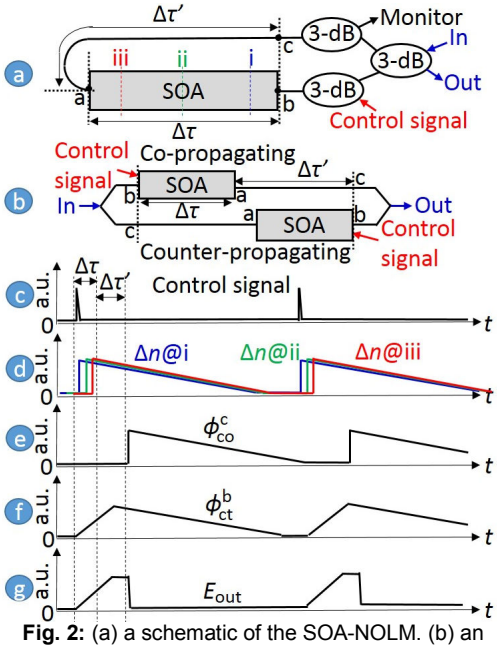

Fig. 2: (a) a schematic of the SOA-NOLM. (b) an equivalent schematic based on a SOA-MZI architecture. Time-domain illustrations of (c) control signal intensity, (d) XGM-induced phase responses at different positions in SOA, (e) phase of the co-propagating signal at 'c', (f) phase of the counter-propagating signal at 'b', and (g) interference-induced intensity switch effect at the output.

propagating signals when passing through the SOA can be regarded as the time-domain integration of the XGM-induced phase responses that the signals undergo at all positions of the SOA. Combining this SOA phase change process and the time delay difference between the counter-propagating signals, the output of the device can be expressed by

$$E_{out}(t) = \gamma E_{in}(t)[\exp(j\phi^{b}_{ct}(t)) - \alpha \exp(j\phi^{c}_{co}(t))]$$
$$= \gamma E_{in}(t)[\exp(j\phi^{b}_{ct}(t)) - \alpha \exp(j\phi^{a}_{co}(t+\Delta\tau'))] \quad (1)$$

where E represents the field amplitude of the signal, α is an amplitude weight factor mainly determined by the coupling coefficient of the coupler, γ is a complex coefficient showing the overall gain and phase shift of the device, $\Delta\tau$' is the time delay determined by the position of the SOA as depicted in Fig. 2b, and the phases, ϕ, of the counter-propagating signals are given by

$$\phi^{a}_{co}(t) = \eta \int_{0}^{\Delta\tau} \Delta n(\tau - \Delta\tau)d\tau + \phi^{b}_{co}(t - \Delta\tau) \quad (2)$$

$$\phi^{b}_{ct}(t) = \frac{\eta}{2} \int_{0}^{2\Delta\tau} \Delta n(\tau - \Delta\tau)d\tau + \phi^{a}_{ct}(t - \Delta\tau). \quad (3)$$

with 'co' and 'ct' referring to 'co-propagating' and 'counter-propagating' respectively, 'a' and 'b' indicating the positions of the output as shown in Fig. 2b, $\Delta\tau$ is the time delay of the SOA, Δn is the XGM-induced phase response at any position of the SOA, and η is a so-called nonlinear-effect coefficient which is determined by the SOA physical properties and in practice can be varied by changing the bias current. Figure 2e and 2f illustrate the output phases of the counter-propagating signals. Figure 2g shows the resulting intensity switching effect caused by the destructive interference as described in Eq. (1). When the control pulse width is much shorter than $\Delta\tau$ and the effect of SOA saturation time is negligible, the rising edge of the switch gate is mainly governed by the phase rising edge of the counter-propagating signal (Fig. 2e), having a duration of $2\Delta\tau$ due to the integration process in Eq. (3); while the falling edge of the switch gate is mainly governed by the phase rising edge of the co-propagating signal (Fig. 2f) that is delayed by the loop roundtrip delay, $\Delta\tau + \Delta\tau$', and has a duration equal to that of the control pulse. This also means that in the case of short control pulse ($<< \Delta\tau$) and the SOA covering nearly half the loop the switching gate has a width approximately equal to the loop roundtrip delay, which is ≈ 23 ps in this work. Based on the mechanism described above, an optical sampler can be implemented when a periodic train of such short pulses are used as the control signal, where the sampling

rate is controlled by the pulse repetition rate.

Experimental demonstration

For the experimental demonstration, we forward-biased the SOA at a saturation current around 200 mA, giving a current density about 7 kA/cm^2 and a small signal gain of 8 dB. The control signal was a train of 1552-nm 5-ps pulses at 10 Gpulses/s, with an average power of 3 dBm at the input of the SOA. For the probe signal, we first applied a CW light at a wavelength of 1546 nm, with a power of -3 dBm at the input of the SOA. This choice of control and probe signal powers maximizes the switching extinction ratio. Figure 3 shows the detected probe signals at 'Port 3' and 'Port 1' (Fig. 1a). The output signal reflected back from 'Port 1' was obtained by means of an optical circulator. Before the detection using a 40-GHz DC-coupled photodiode (Discovery DSO-40s), a 150-GHz-passband optical filter was used to remove the control pulses and suppress the amplified spontaneous emission power from the SOA (-40 dBm/nm), and the average optical powers of the two ports were amplified to -1 dBm. In the result, 'Port 1' and 'Port 3' show complementary signal amplitudes, agreeing with the interference process in the device working principle. 'Port 1' shows the sampling gate's window function. This has a window extinction about 7 dB and a width of ≈ 30 ps. The limited extinction is mainly due to the coupling coefficient offset of the fabricated coupler, which can be improved when having a better coupler performance. The sampling gate window width agrees with device principle explained above. The additional width exceeding the 23-ps loop roundtrip delay is mainly because the control pulse itself has a width of 5 ps and the photodiode associated with the scope gives a rise-time of 26 ps, causing sampling gate window broadening.

As another demonstration of the sampling function, we changed the probe signal from a CW light to an intensity-modulated optical signal. The modulating signal was generated by processing a 5 x 10 Gbaud OOK-OFDM signal through a 9-point Fourier transform, the result of which provides a modulating signal waveform characterized by eye-diagrams as shown in Fig. 4a and 4b, having an eye opening of 30 ps at an

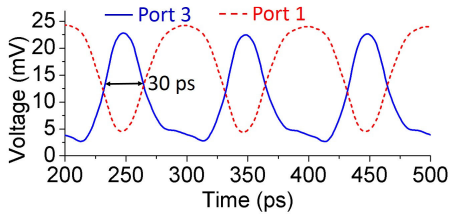

Fig. 3: Detected output signals of the chip when using a 10-GHz-rate, 5-ps-width pulse train as the control signal (Port 4) and a CW light as the input signal (Port 1).

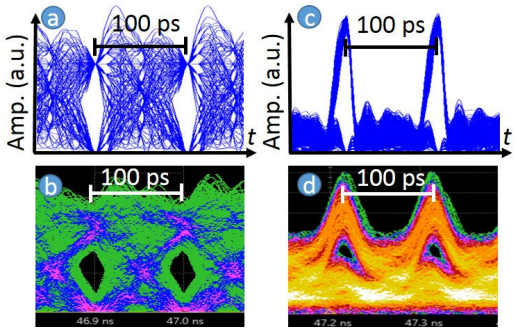

Fig. 4: (a, b) calculated and measured eye-diagrams of the input signal before optical sampling, (c, b) those of the output signal after optical sampling.

interval of 100 ps. When applying this modulated optical signal to the device input and having its eye positions time-aligned with the 10Gpulses/s control pulses, the device output provided a sampled version of the input. The eye-diagrams of the detected output are shown in Fig. 4c and 4d. Evidently, the eyes are preserved while suppression occurs elsewhere. While this experiment shows a limited performance due to fluctuations in signal timing and power (imperfections in the lab setup), the result verifies the optical sampler function of the device.

Conclusion

We have designed an on-chip optical sampler using an integrated SOA-NOLM. It has a size of 2 × 1.2 mm^2 and shows a sampling gate extinction ≈ 7 dB and a width ≈ 30 ps.

Acknowledgements

We acknowledge support from Australian Research Council grants FL13100041 and CE110001018.

References

[1] A. J. Lowery *et al*., "All-optical OFDM transmitter design using AWGRs and low-bandwidth modulators," Opt. Express **19**, 15696 (2011).

[2] M. Saruwatari *et al*., "All-optical signal processing for terabit/second optical transmission," IEEE J. Select. Topics Quantum Electron. **6**, 1363 (2000).

[3] S. Shimizu *et al*., "Demonstration and performance investigation of all-optical OFDM systems based on arrayed waveguide gratings," Opt. Express **20**, (2012).

[4] S. Fischer *et al*., "All-optical sampling with a monolithically integrated Mach-Zehnder interferometer gate," Opt. Lett., **26**, 626 (2001).

[5] K. E. Stubkjaer *et al*., "Semiconductor optical amplifier-based all-optical gates for high-speed optical processing," IEEE J. Sel. Top. Quant. Electron. **6**, 1428 (2000).

[6] J. P. Sokoloff *et al*., "A terahertz optical asymmetric demultiplexer (TOAD)," **23**, 787 (1993).

[7] G. Gilardi *et al*., "Generic InP-based integrated technology: present and prospects," Progress in Electromagnetic Research **147**, 23 (2014).

